Uterine double-conditional inactivation of *Smad2* and *Smad3* in mice causes endometrial dysregulation, infertility, and uterine cancer

Maya Kriseman[a,b], Diana Monsivais[a,c], Julio Agno[a], Ramya P. Masand[a], Chad J. Creighton[d,e], and Martin M. Matzuk[a,c,f,g,h,1]

[a]Department of Pathology and Immunology, Baylor College of Medicine, Houston, TX 77030; [b]Reproductive Endocrinology and Infertility, Baylor College of Medicine/Texas Children's Hospital Women's Pavilion, Houston, TX 77030; [c]Center for Drug Discovery, Baylor College of Medicine, Houston, TX 77030; [d]Department of Medicine, Baylor College of Medicine, Houston, TX 77030; [e]Dan L. Duncan Comprehensive Cancer Center, Baylor College of Medicine, Houston, TX 77030; [f]Department of Molecular and Cellular Biology, Baylor College of Medicine, Houston, TX 77030; [g]Department of Molecular and Human Genetics, Baylor College of Medicine, Houston, TX 77030; and [h]Department of Pharmacology and Chemical Biology, Baylor College of Medicine, Houston, TX 77030

Contributed by Martin M. Matzuk, December 6, 2018 (sent for review April 30, 2018; reviewed by Milan K. Bagchi and Thomas E. Spencer)

SMAD2 and SMAD3 are downstream proteins in the transforming growth factor-β (TGF β) signaling pathway that translocate signals from the cell membrane to the nucleus, bind DNA, and control the expression of target genes. While SMAD2/3 have important roles in the ovary, we do not fully understand the roles of SMAD2/3 in the uterus and their implications in the reproductive system. To avoid deleterious effects of global deletion, and given previous data showing redundant function of *Smad2* and *Smad3*, a double-conditional knockout was generated using progesterone receptor-cre (*Smad2/3 cKO*) mice. *Smad2/3* cKO mice were infertile due to endometrial hyperproliferation observed as early as 6 weeks of postnatal life. Endometrial hyperplasia worsened with age, and all *Smad2/3* cKO mice ultimately developed bulky endometrioid-type uterine cancers with 100% mortality by 8 months of age. The phenotype was hormone-dependent and could be prevented with removal of the ovaries at 6 weeks of age but not at 12 weeks. Uterine tumor epithelium was associated with decreased expression of steroid biosynthesis genes, increased expression of inflammatory response genes, and abnormal expression of cell cycle checkpoint genes. Our results indicate the crucial role of SMAD2/3 in maintaining normal endometrial function and confirm the hormone-dependent nature of SMAD2/3 in the uterus. The hyperproliferation of the endometrium affected both implantation and maintenance of pregnancy. Our findings generate a mouse model to study the roles of SMAD2/3 in the uterus and serve to provide insight into the mechanism by which the endometrium can escape the plethora of growth regulatory proteins.

TGF β signaling | uterine hyperplasia | endometrial cancer | female reproduction | knockout mouse

The endometrium is a dynamic tissue that is continuously changing in response to hormonal expression and requires a delicate interplay of cellular and molecular events. Defects in the regulation of the endometrium can have serious implications in women. About 10% of women (~6.1 million) in the United States aged 15–44 y have difficulty getting pregnant or staying pregnant (1), with defects in the endometrium being implicated in cases of poor implantation, pregnancy loss, and placental abnormalities. Endometrial hyperplasia changes the uterine environment, thereby affecting implantation and pregnancy, and can progress to uterine cancer, the most commonly diagnosed gynecological cancer in the United States, affecting ~50,000 women each year (2). However, fertility-sparing progesterone therapy for early endometrial carcinoma and atypical complex endometrial hyperplasia only results in resolution in ~40–80% of patients, with a recurrence risk of ~20–40% (3–7). Therefore, understanding the mechanism by which the endometrium is regulated is prudent for both fertility and cancer therapy.

Several regulatory proteins, growth factors, and their receptors (8–12) have been studied and identified to play an important role in endometrial function. Notably, members of the transforming growth factor β (TGF β) family are involved in many cellular processes and serve as principal regulators of numerous biological functions, including female reproduction. Previous studies have shown the TGF β family to have key roles in ovarian folliculogenesis and ovulation (13, 14), decidualization (15, 16), implantation (17, 18), placentation (17, 19), uterine receptivity (15), and uterine development (20, 21), with disruption in the TGF β family causing reproductive diseases and cancer (22–25).

SMAD2 and SMAD3 are downstream proteins in the TGF β signaling family that are important in translocating signals to the nucleus, binding DNA, and regulating the expression of target genes. Previous studies in mouse models have shown that deletion of the type 1 TGF β receptor (ALK5) upstream of SMAD2/3 results in fertility defects (17, 26) and that when deletion is combined with PTEN inactivation (a tumor suppressor),

Significance

Endometrial hyperplasia, a result of unopposed estrogen, changes the uterine environment. This overgrowth of uterine lining can progress to uterine cancer and disrupt uterine receptivity and implantation. However, fertility-preserving progesterone therapy for early endometrial carcinoma and atypical endometrial hyperplasia does not always result in resolution. Therefore, a better understanding of the mechanisms by which the endometrium is regulated is prudent for both fertility and cancer therapy. We generated a conditional knockout of *Smad2/3* in the uterus and demonstrated that *Smad2/3* plays a critical role in the endometrium, with disruption resulting in pubertal-onset uterine hyperplasia and, ultimately, lethal uterine cancer. Our findings provide a mouse model to investigate transforming growth factor-β signaling in reproduction and cancer and advance our understanding of endometrial pathogenesis.

Author contributions: M.K., D.M., and M.M.M. designed research; M.K., D.M., and J.A. performed research; M.K., D.M., R.P.M., C.J.C., and M.M.M. analyzed data; and M.K., D.M., and M.M.M wrote the paper.

Reviewers: M.K.B., University of Illinois; and T.E.S., University of Missouri.

Conflict of interest statement: D.M. and T.E.S. are coauthors on a 2015 Commentary article.

Data deposition: The RNA sequencing data reported in this paper have been deposited in the Gene Expression Omnibus, https://www.ncbi.nlm.nih.gov/geo (accession no. GSE112664).

See Commentary on page 3367.

[1]To whom correspondence should be addressed. Email: mmatzuk@bcm.edu.

This article contains supporting information online at www.pnas.org/lookup/suppl/doi:10.1073/pnas.1806862116/-/DCSupplemental.

Published online January 16, 2019.

it promotes aggressive endometrial cancer progression (27). Likewise, the role of SMAD2/3 in the ovary has previously been characterized, showing defects in follicular development, ovulation, and cumulus cell expansion (14). In humans, abnormal expression of TGF β receptors has also been shown in endometrial cancer (28, 29), with SMAD2/3 specifically being implicated in several human tumors, including colon (24) and pancreas (30) tumors. Despite the growing abundance of TGF β pathway literature, we do not fully understand the roles of SMAD2/3 in the uterus and their implications in fertility and uterine cancer.

Mouse models are powerful tools that allow us to investigate gene function in vivo and provide us with a better understanding of uterine regulation. Global knockout of *Smad2* is embryonic lethal in mice (31, 32), whereas global knockout of *Smad3* results in ultimate death postnatally (33, 34). Therefore, conditional deletion of *Smad2/3* in the uterine stroma and endometrium was obtained using a progesterone receptor-cre (*Pgr-cre*) mouse model (35).

Deletion of uterine *Smad2/3* led to uterine hyperplasia, which resulted in infertility and eventual lethal uterine tumor formation. Therefore, elucidating the role of SMAD2/3 in the endometrium will uncover the mechanism by which the endometrium can escape the abundance of growth regulatory proteins.

Results

Generation of *Smad2/3* Double-Conditional Knockout Mice and Smad2/3 Expression in the Uterus. Because complete loss of *Smad2* results in embryonic lethality (31, 32) and to avoid deleterious effects of *Smad3* deletion (33, 34), we generated a conditional knockout (cKO) mouse model. Given previous data showing the redundant functions of SMAD2 and SMAD3 (14, 36, 37), and notably in the reproductive tract (14), a double-cKO mouse model was generated. *Smad2* and *Smad3* double-cKO mice were previously generated using the Cre-loxP system, where loxP sites were introduced to flank exons 9 and 10 for *Smad2* ($Smad2^{flox/flox}$) (14, 38) and exons 2 and 3 for *Smad3* ($Smad3^{flox/flox}$) (14) (*SI Appendix*, Fig. S1*A*). To obtain tissue-specific deletion in this study, $Smad2^{flox/flox}$ and $Smad3^{flox/flox}$ females were mated to males expressing the *Pgr-cre* knock-in allele. Previous studies indicated that Pgr-cre is expressed postnatally in the ovary, uterus, oviduct, mammary gland, and pituitary gland (35). Efficiency of Pgr-cre–mediated recombination in the female reproductive system was previously confirmed (17). Using this mating strategy $Smad2^{flox/flox}$;$Smad3^{flox/flox}$;*Pgr-cre* (herein called *Smad2/3* cKO) mice were produced (*SI Appendix*, Fig. S1*B*).

Mice were genotyped by PCR analyses of genomic tail DNA using specific primers (*SI Appendix*, Table S1). Efficiency of Smad2/3 deletion was confirmed by real-time quantitative PCR (qPCR). Significant reduction of the *Smad2* and *Smad3* mRNA levels was detected in the uterus (*SI Appendix*, Fig. S1*C*) and the oviducts (*SI Appendix*, Fig. S2*A*), with no significant reduction seen in the ovaries (*SI Appendix*, Fig. S2*B*). To evaluate the possible effects of *Smad2* and *Smad3* deletion on the hypothalamic–pituitary–ovarian–uterine axis, we evaluated the hormonal profiles of the mutant mice. To do so, we analyzed the serum of control and *Smad2/3* cKO female mice for the circulating levels of follicle-stimulating hormone (FSH) and luteinizing hormone (LH) at 6 and 12 wk. There were no differences in the levels of FSH or LH (*SI Appendix*, Fig. S3 *A–D*) at either 6 or 12 wk. This lack of effect on pituitary function is supported by a previous study by Matzuk et al. (39), which showed that deletion of ACVR2A (a type 2 receptor that signals through SMAD2/3) suppressed FSH levels in female mice, suggesting that if our *Smad2/3* cKO mouse model affected pituitary function, it would be reflected by an aberration in the pituitary hormones.

***Smad2/3* cKO Female Mice Exhibit Infertility but Have Normal Ovarian Function.** To evaluate the fertility of *Smad2/3* cKO female mice, we performed a continuous breeding study for control ($Smad2^{flox/flox}$; $Smad3^{flox/flox}$) and *Smad2/3* cKO female mice (Table 1). We mated 6-wk-old female mice ($n = 12$ for control and $n = 11$ for *Smad2/3* cKO) with known fertile WT male mice for 6 mo. The 12 control females had normal breeding activity during the test period. In contrast, ablation of uterine *Smad2/3* led to sterility in 10 of the 11 females tested. The remaining female had one initial litter of two pups in the first month of breeding, with no subsequent litters or offspring. Vaginal plugs were observed at similar frequencies between the two genotypes, which eliminated the possibility of abnormal mating behavior. Compared with the controls, uteri from the *Smad2/3* cKO mice had fewer implantation sites (Fig. 1*A*), with a trend toward smaller weight per implantation site (Fig. 1*B*). Hemorrhagic implantation sites were also noted at 10.5 d post coitum (dpc) in the *Smad2/3* cKO mice, suggesting poor placentation.

Table 1. Six-month mating study

Genotype	Females	Litters	Pups per litter	Litters per month
Control	12	65	6.4 ± 1.9	0.8 ± 0.3
Smad2/3 cKO	11	1	2*	0.01

*One female had one litter.

In Pgr-cre transgenic mice, Cre is also expressed in the granulosa cells of preovulatory follicles (35); we therefore examined ovarian function in the control and *Smad2/3* cKO mice. In histological analyses of adult female ovaries, the *Smad2/3* cKO mice exhibited normal ovarian follicles compared with control mice, with corpora lutea observed in both (*SI Appendix*, Fig. S4*A*). Likewise, superovulation of 3-wk-old mice showed no significant difference in the number of oocytes released (*SI Appendix*, Fig. S4*B*). Therefore, ovarian architecture and functional ovulation were normal in the *Smad2/3* cKO mice.

***Smad2/3* cKO Female Mice Exhibit Uterine Hyperplasia and Hyperproliferation.** Because the fertility defects were not due to an ovarian origin and to further elucidate the roles of SMAD2/3 in the female reproductive system, histological analyses were performed on the uteri of control and *Smad2/3* cKO mice at various time points. Immunostaining of 4-wk-old uteri with smooth muscle actin (SMA) and cytokeratin 8 (CK8), markers of the myometrial and epithelial layers of the uterus, respectively, showed no difference in structure (*SI Appendix*, Fig. S5 *A* and *B*). However, staining with forkhead box A2 (FOXA2), a glandular marker, showed a larger number of uterine glands, with more irregular appearing glands in the *Smad2/3* cKO uteri indicating an early role of SMAD2/3 in uterine gland formation (*SI Appendix*, Fig. S5 *C* and *D*). By 6 wk of postnatal life, disruption of the normal endometrium was seen, with notable continued hyperplasia at 9 wk of life (Fig. 2). Fig. 2 shows the uteri of control and *Smad2/3* cKO mice stained with E-cadherin, a marker of the uterine luminal and glandular epithelium (Fig. 2 *A–D*), at 6 and 9 wk of age. In Fig. 2 *E–H*, immunostaining with SMA and CK8 indicated that endometrial hyperproliferation in the *Smad2/3* cKO mice was detectable beginning at 6 wk of age, with no defects or invasion into the myometrial compartment.

Since the double deletion of *Smad2* and *Smad3* genes led to uterine compartment-specific effects, RNA expression was performed on control mice at the onset of puberty as well as during proestrus and diestrus [time point for highest (estrogen-dominant) and lower estrogen expression (progesterone-dominant)] to further ascertain how signaling may affect uterine function. *Smad3* was expressed equally in the epithelial and stroma/myometrium compartments of the uterus at puberty as well as during diestrus and proestrus (*SI Appendix*, Fig. S6 *D–F*). Expression of *Smad2*, however, was significantly higher in the stroma/myometrium component compared with the epithelium during diestrus and proestrus but not at 6 wk (*SI Appendix*, Fig. S6 *A–C*).

By 12 wk of age, a marked increase in uterine endometrial proliferation (Fig. 3 *A–H*) was observed. E-cadherin immunostaining (Fig. 3 *A–D*) showed the presence of endometrial hyperplasia in the *Smad2/3* cKO mice. Significant up-regulation of

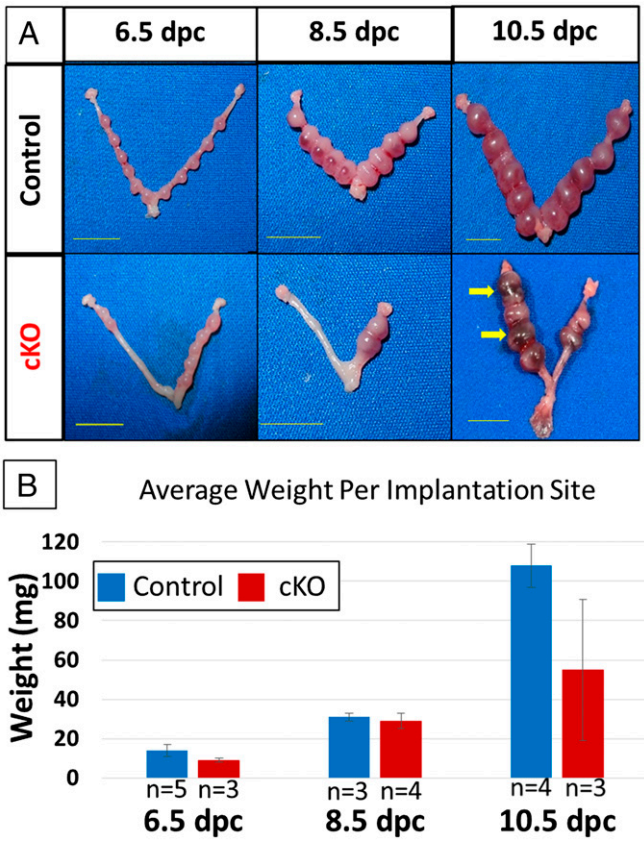

Fig. 1. *Smad2/3* cKO female mice exhibit Infertility. (*A*) SMAD 2/3 cKO mice have fewer implantation sites compared with control mice at 6.5, 8.5, and 10.5 dpc. (Scale bars: 1.0 cm.) (*B*) Trend toward smaller implantation sites. *P* values are 0.11, 0.56, and 0.056 in 6.5-, 8.5-, and 10.5-dpc implantation sites, respectively. Data are presented as mean ± SEM. Yellow arrows indicate hemorrhagic implantation sites.

mRNA levels of cytokeratin 18 (*Krt18*) and E-cadherin (*Cdh1*) (epithelial cell markers) was detected in *Smad2/3* cKO uterus (Fig. 3 *I* and *J*). Similarly, immunostaining with SMA and CK8 showed that the epithelial hyperplasia was contained within the endometrial layer and had not invaded into the underlying myometrium (Fig. 3 *E–H*). Phosphorylated histone H3 (pHH3) visualizes the four phases of mitosis and late G2 and is used as a marker of active cell proliferation (40). Unlimited cell division is a hallmark of carcinogenesis; therefore, pHH3 expression was evaluated in the uteri of control and *Smad2/3* cKO mice. Although pHH3-positive cells were observed in the uteri of control and *Smad2/3* cKO mice, pHH3 immunoreactivity was notably increased in the *Smad2/3* cKO uterus (Fig. 3 *K–N*). Quantification of the monoclonal antibody Ki67, another well-known marker of active cell proliferation (41), in control ($n = 3$) and *Smad2/3* cKO ($n = 3$) mice showed a significantly higher expression of Ki67 in the *Smad2/3* cKO mice (53% vs. 36%; $P = 0.02$).

***Smad2/3* cKO Female Mice Lose Progesterone Receptor Expression, Develop Hormone-Dependent Uterine Tumors, and Die by 8 Mo of Age.** Given that endometrial dysregulation started at the onset of puberty and because the more common type of uterine cancer is due to unopposed estrogen (42), hormonal dependence was suspected to occur in the *Smad2/3* cKO uterus. Significant up-regulation in the expression of estrogen-responsive genes (*Lcn2*, *Muc1*, and *Clca3*) was noted in the *Smad2/3* cKO mouse uteri (Fig. 4 *A–C*). The levels of serum estradiol in control and *Smad2/3* cKO mice at 6 and 12 wk were beneath the level of detection for both groups of mice. Despite no change in expression of *Pgr* or progesterone-responsive genes (*Mig6*, *il13ra2*, *Areg*, *Lrp2*, *Hand2*, and *CoupTFII*) between the control and *Smad2/3* cKO mice (*SI Appendix*, Fig. S7), progesterone receptor (PR) immunostaining showed that PR was absent in the 12-wk-old *Smad2/3* cKO mouse uterus but not in the controls (Fig. 4 *E–H*). PR immunostaining was not significantly decreased in the stroma [66% (control) vs. 44% (cKO); $P = 0.21$]. Interestingly, while serum progesterone levels were the same at 6 wk between control and *Smad2/3* cKO mice, they were noted to be significantly lower at 12 wk in the *Smad2/3* cKO mice (*SI Appendix*, Fig. S3 *E* and *F*). Compared with controls (Fig. 4 *I* and *J*), disordered uterine glandular structures in the *Smad2/3* cKO mice were visualized by immunohistochemistry of the glandular marker FOXA2 (Fig. 4 *K* and *L*), with a corresponding increase in *Foxa2* gene expression in the *Smad2/3* cKO mice relative to the controls (Fig. 4*D*).

Unlike control mouse uterus (Fig. 5*B*), the *Smad2/3* cKO mice went on to develop bulky uterine cancers (Fig. 5 *A* and *C*). In comparison to normal kidneys (Fig. 5*D*), while there was no histological evidence of disease, the compression of the large uterine mass against the vasculature caused significant dilation of the kidney (hydronephrosis, $n = 4$) (Fig. 5*E*). Mass effect also resulted in sequelae such as labial mass protrusion ($n = 5$) (Fig. 5*H*). The uterine cancers exhibited a loss of lumen with chaotically growing endometrial epithelial cells invading throughout the entire myometrium and the serosal surface of the uterus with no normal uterine architecture remaining (Fig. 5 *I* and *J*).

Compared with control mice (Fig. 5*F*), the cancers were noted to metastasize to the lungs ($n = 9$) (Fig. 5*G*), but to no other tissue. The lung metastasis showed nodules with proliferation of malignant glands distorting normal lung architecture similar to

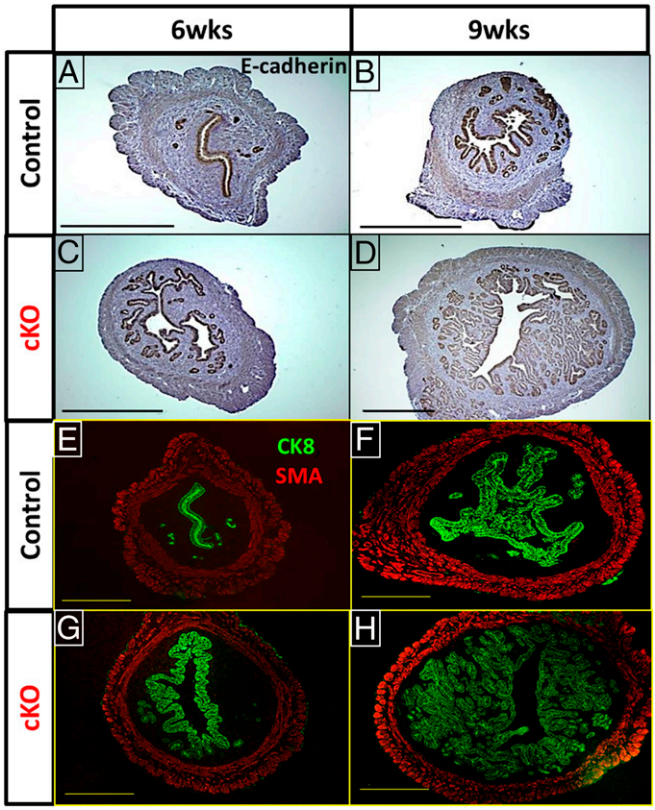

Fig. 2. Disordered and hyperplastic epithelium in cKO mice is observed as early as 6 wk of age. Uterine cross-sections of 6-wk-old control and cKO mice stained with E-cadherin (*A–D*) or double-stained with CK8 and SMA (*E–H*). (Scale bars: 0.5 mm.)

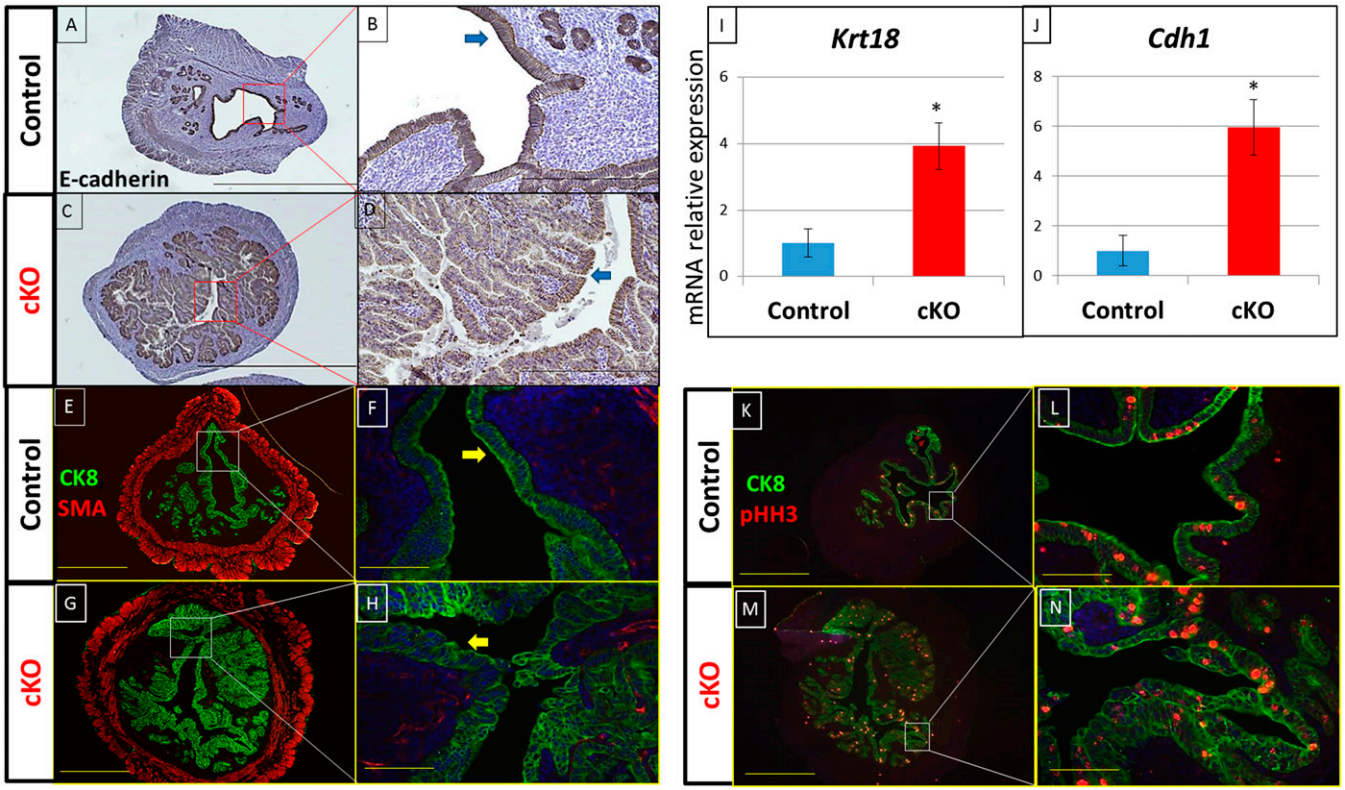

Fig. 3. Uterine hyperplasia and hyperproliferation in 12-wk-old *Smad2/3* cKO uteri. (*A–D*) Immunostaining with E-cadherin (a marker of uterine luminal and glandular epithelium) showing increased epithelial proliferation in cKO mice compared with control mice. Blue arrows (*B* and *D*) indicate the luminal uterine epithelium. (*E–H*) Immunofluorescence (IF) staining with SMA (a myometrial marker) and CK8 (an epithelial marker) showing epithelial hyperplasia contained within the endometrial layer with no invasion into the myometrium. Yellow arrows (*F* and *H*) indicate the luminal uterine epithelium. (*I* and *J*) qPCR showing significant up-regulation of epithelial markers (*Krt18* and *Cdh1*) in *Smad2/3* cKO mice. (*K–N*) Immunostaining with CK8 and pHH3 (marker of hyperproliferation) showing increased expression of pHH3 in the cKO mice as compared with the controls. *$P \leq 0.05$ compared with controls. (*C*) IF staining with CK8 and pHH3 (a cell proliferation marker) showing increased proliferation in *Smad2/3* cKO mice compared with control mice. (Scale bars: *A*, *C*, *E*, *G*, *K*, and *M*, 0.5 mm; *B*, *D*, *F*, *H*, *L*, and *N*, 100 μm.) Cdh1, E-cadherin; Krt18, cytokeratin 18. Data are presented as mean ± SEM [$n = 5$ (control) and $n = 4$ (cKO)].

the morphology noted in the uterus (Fig. 5 *K* and *L*). All of the *Smad2/3* cKO mice died by 34 wk of age, with a 50% survival rate of 26.5 wk (Fig. 5*M*).

***Smad2/3* cKO Cancer Phenotype Can Be Avoided if Ovaries Are Removed at Onset of Puberty.** To further confirm hormonal dependence, ovaries were removed from *Smad2/3* cKO mice to see if cancer formation could be prevented. Ovaries were removed at the onset of puberty at 6 wk of age, approximately the start of uterine hyperplasia, and at 12 wk of age, around the time of marked uterine hyperplasia. Mice were subsequently dissected at 6 mo of age and compared with WT (Fig. 6*A*) and cKO non-ovariectomized controls (Fig. 6*D*). Ovary removal at 6 wk of age prevented the phenotype of both hyperplasia and tumor formation (Fig. 6*B*). However, if the ovaries were removed at 12 wk of the age, the mice continued to develop uterine cancer (Fig. 6*C*), as evidenced both grossly and histologically. However, the severity of the uterine cancer phenotype varied in the mice ovariectomized at 12 wk of age: Three of seven mice died from their cancer by 6 mo. The remaining mice had varying degrees of disease at the time of dissection. Removal of ovaries at 6 wk (*SI Appendix*, Fig. S8 *A* and *B*) also prevented the loss of PGR protein expression but not removal at a later time point (*SI Appendix*, Fig. S8 *C* and *D*). Because ovariectomy suggests estrogen dependence but does not indicate causality, estradiol was reintroduced into the ovariectomized control and *Smad2/3 cKO* mice. Given that a significant phenotype was already noted after 3 wk postpuberty, 100 ng of estradiol was injected daily for 3 wk into control and *Smad2/3 cKO* ovariectomized mice. Both developed hyperplasia due to the unopposed estrogen, but the *Smad2/3 cKO* phenotype was more impressive, with an increased presence of glands and hyperplastic epithelium (*SI Appendix*, Fig. S9)

***Smad2/3* cKO Mice Demonstrate Abnormal Expression of Genes Involved in Inflammation, Cell Cycle Checkpoint, Migration, Steroid Biosynthesis, and SMAD1/5-Driven Genes.** We performed RNA sequencing to identify the gene expression differences between the uterine epithelium of control and *Smad2/3* cKO mice. To avoid the confounding factors triggered by hormonal changes throughout the estrus cycle, we chose to profile the uterine epithelium from mice at 0.5 dpc. Global gene expression profiles of *Smad2/3* cKO versus control mice were analyzed. We found 1,227 features with $P < 0.01$ (*t* test, cKO versus control) and fold change > 1.4 (Dataset S1*A*). Gene ontology analysis was performed for the most up-regulated and down-regulated genes (Dataset S1*B*).

There was significant up-regulation in SMAD1/5 gene targets [inhibitors of DNA binding/inhibitors of differentiation (Id) protein family *Id1–4*], which have been associated with angiogenesis and tumor progression in different gynecological cancers (43–45). This indicates that in the absence of SMAD2/3, the SMAD1/5 signaling pathway is overactivated, which has been previously reported to occur in other cell types and organisms (46–48).

We also observed significant differences in the genes encoding proteins involved in cell cycle checkpoints and cell migration in the *Smad2/3* cKO mice compared with the controls. For example, there was decreased mRNA expression in *Slit2* [involved in

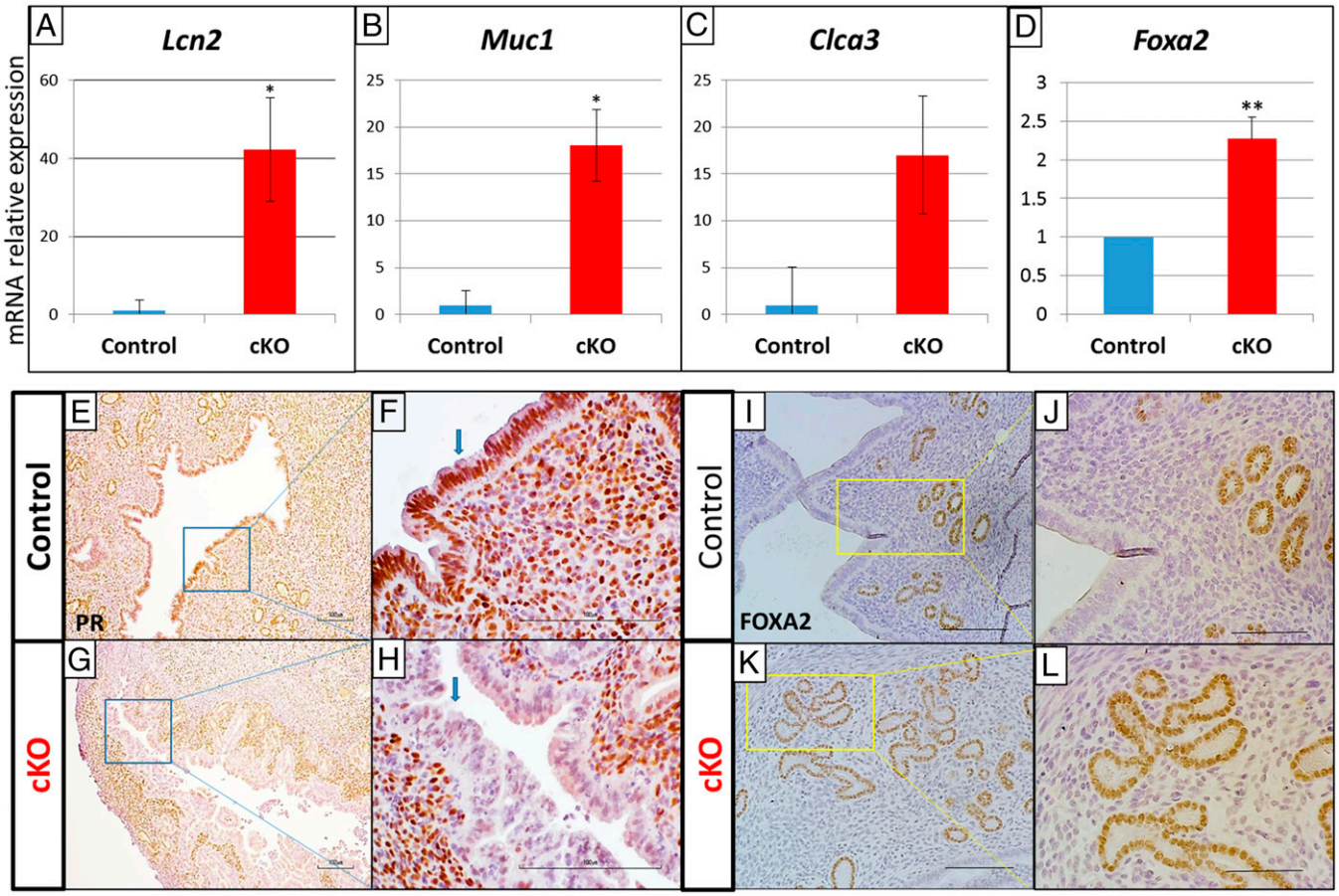

Fig. 4. *Smad2/3* cKO 12-wk-old female mice express high levels of estrogen-responsive genes, have an increase in uterine gland formation, and lose PR expression. (*A–C*) qPCR showing estrogen markers significantly up-regulated in *Smad2/3* cKO mice. *Clca3*, chloride channel accessory; *Lcn2*, lipocalin 2; *Muc1*, Mucin1. (*D*) qPCR showing *Foxa2* (a glandular marker) significantly up-regulated in *Smad2/3* cKO mice. Data are presented as mean ± SEM [$n = 5$ (control) and $n = 4$ (cKO)]. *$P \leq 0.05$; **$P \leq 0.01$. Immunohistochemistry (IHC) shows nuclear PR expression in the epithelium of control mice at low (*E*) and high (*F*) power and a loss of PR expression in the epithelium of *Smad2/3* cKO mice at low (*G*) and high (*H*) power. Blue arrows indicate the luminal uterine epithelium. IHC of FOXA2 (a glandular marker) shows normal endometrial glands at low (*I*) and high (*J*) power and increased and irregular-shaped glands in a cKO mouse at low (*K*) and high (*L*) power. (Scale bars: *I* and *K*, 0.5 mm; *E–H*, *J*, and *L*, 100 μm.)

molecular guidance in cellular migration (49)] and *Bcl2* [apoptosis regulator (50)] and increased expression of *Agr2* [involved in cell migration and metastasis (51–54)] and *Cks1b* [cell cycle G1/S and G2/M DNA damage checkpoints (55–57)]. These findings support the hyperproliferative and metastatic capacity of the endometrial tumors observed in the *Smad2/3* cKO mice.

The steroid biosynthetic pathway is composed of a group of transporters and enzymes whose main role is to import cholesterol and subject it to a series of enzymatic reactions to yield steroid hormones (58). The steroid biosynthetic pathway controls not only the circulating levels of hormones in an organism but also the local steroid concentrations at the tissue level (59). For example, in women, local estradiol concentrations are five- to eightfold higher in endometrial tissues compared with circulating levels of estradiol in the serum. Significant down-regulation in several genes [*Ces1d*, *Cyp51*, *Fdft1*, and *Cyp21a1* (58, 60–62)] involved in steroid/cholesterol biosynthesis was noted in the *Smad2/3* cKO epithelium. Validation of these genes in mouse tissues by qPCR confirmed these findings (Fig. 7), indicating that local steroid biosynthesis is altered in the *Smad2/3* cKO tissues.

TGF β is involved in the regulation of various cell types of the immune system important in inflammatory response, such as macrophages, neutrophils, and cytokines (63, 64). Conditional deletion of TGF βs and the downstream signaling proteins, SMAD2 and SMAD3, has resulted in a profound increase in inflammatory response leading to death (33, 37, 65) In our model, we observed a significant increase in inflammatory response genes (*Crispld2* and *Ccl20*). *Ccl20* encodes a chemokine that has been implicated in tumor growth and invasiveness (66). Surprisingly, *Crispld2* has been shown to suppress inflammation (67, 68), which is contrary to our findings, and has even been found to be highly expressed in some human endometrial tumors (69) (https://www.proteinatlas.org/ENSG00000103196-CRISPLD2/pathology).

Discussion

In this study, we conditionally deleted SMAD2 and SMAD3 using *Pgr*-cre, which led to dramatic pathological changes in the epithelial layers of the uterus. *Smad2/3* cKO mice displayed abnormal glandular tissue at 4 wk of life, indicating an important role of SMAD2/3 in early glandular formation. *Smad2/3* cKO mice develop uterine hyperplasia after the onset of puberty, and this hyperplasia progresses to aggressive uterine cancers with associated metastasis to the lungs. Due to such early hyperplasia, there is a disruption in normal implantation and continuation of pregnancy, resulting in sterility of these mice. This was evidenced in the trend toward decreased number and weight of *Smad2/3* cKO implantation sites in comparison to controls, as well as hemorrhagic implantation sites noted at 10.5 dpc. A delayed onset of the hyperplasia phenotype is likely the reason why one mouse was able to deliver one litter of two pups, which was

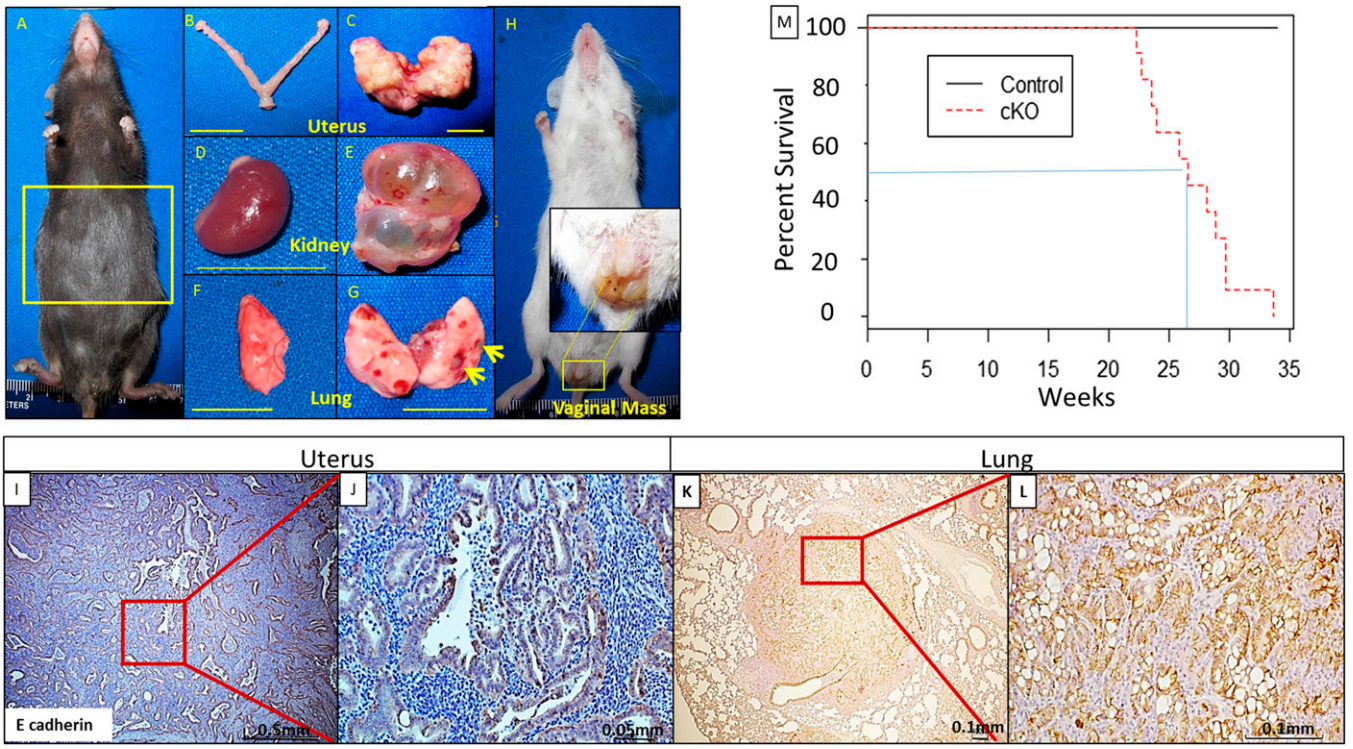

Fig. 5. *Smad2/3* cKO female mice develop bulky endometrioid-type tumors with lung metastases and die by 34 wk of age. (*A*) *Smad2/3* cKO female mouse at ∼5 mo of age. (*B*) Gross dissection of control mouse uterus at 5 mo of age. (*C*) Gross dissection of cKO mouse showing a uterine tumor at 5 mo of age. (*D*) Gross dissection of control kidney. Hydronephrosis (*E*) and labial mass protrusion (*H*) result from mass effect of a uterine tumor. Gross dissection of control (*F*) and cKO (*G*) lung is shown. Yellow arrows point at sites of metastasis. (Scale bars: 1 cm.) (*I* and *J*) Immunostaining with E-cadherin (an epithelial marker) of a uterine tumor showing loss of normal architecture and overabundance of glandular tissue. (*K* and *L*) Immunostaining with E-cadherin of lung metastasis showing a nodule with proliferation of malignant glands distorting normal morphology. (*M*) Kaplan–Meier survival curve showing 100% mortality by 34 wk of age, with 50% survival at 26.5 wk.

confirmed by that animal's inability to have additional litters and its subsequent development of uterine cancer.

This study showed that the function of SMAD2/3 in the uterus was hormonally dependent. While previous work (70) has shown that estrogen causes SMAD2/3 degradation and has proposed that it inhibits cancer metastasis, this work shows that the absence of SMAD2/3 does not inhibit metastasis and that the presence of SMAD2/3 is critical for an appropriate response of the endometrium to hormones. One possible mechanism of tumor formation in the *Smad2/3* cKO mice presented here could be due to the loss

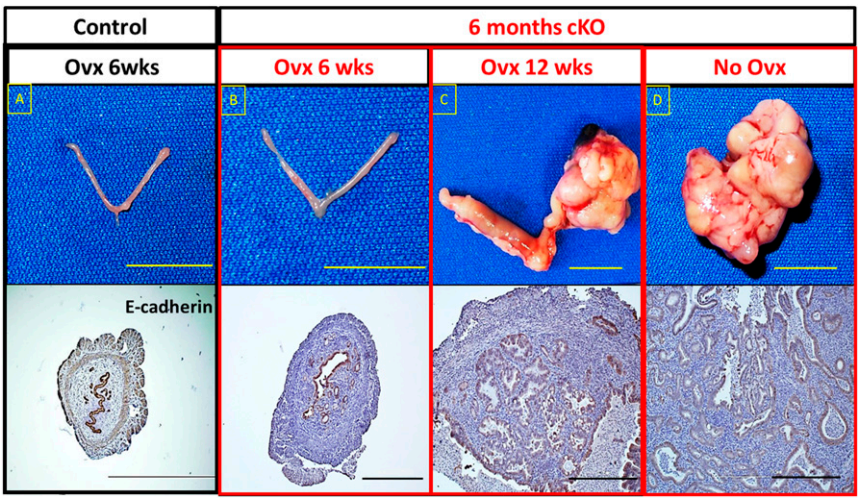

Fig. 6. Smad2/3 cKO cancer phenotype is avoided if ovaries are removed at the onset of puberty. Mice were killed at 6 mo of age. (*A*) Control ovariectomized (Ovx) mouse showing normal gross pathology and uterine histology. (*B*) *Smad2/3* cKO mouse after Ovx at 6 wk showing normal gross pathology and uterine histology. (*C*) *Smad2/3* cKO mouse after Ovx at 12 wk showing formation of uterine tumor grossly and increased glandular formation/disruption of normal uterine architecture on histology. (*D*) *Smad2/3* cKO without Ovx showing a large bulky uterine tumor and advanced uterine cancer with complete loss of luminal epithelium on histology. [Scale bars: *Top* (panel: gross specimen), 1 cm; *Bottom* (panel: histology), 100 μm.]

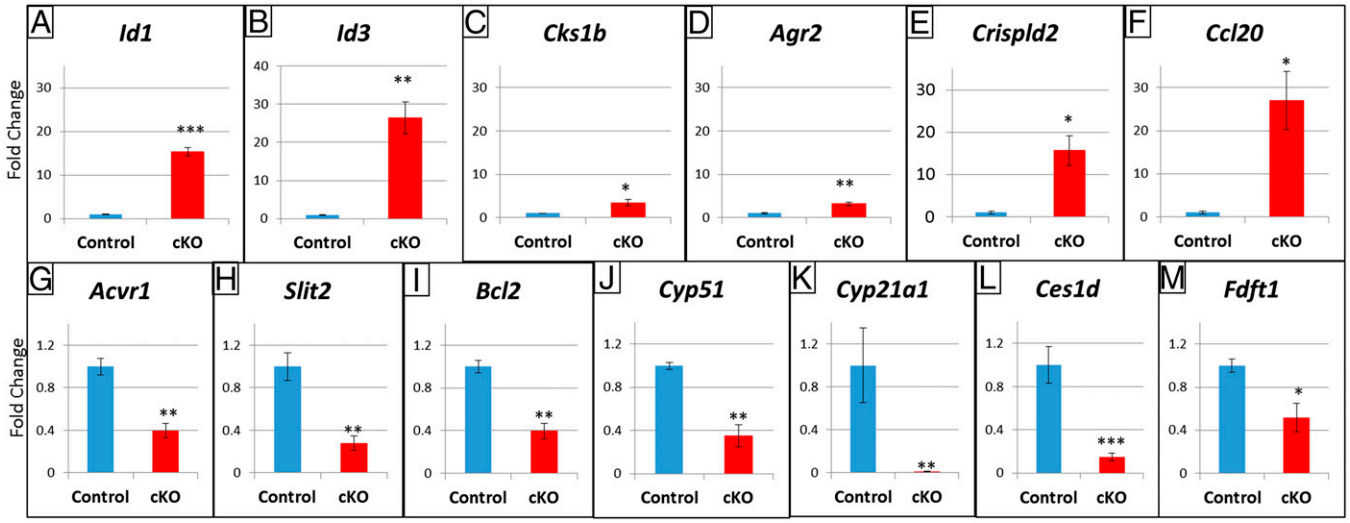

Fig. 7. *Smad2/3* cKO causes abnormal expression in genes involved in inflammation, cell cycle checkpoints and migration, the steroid biosynthesis pathway, and SMAD1/5-driven genes. qPCR validation of RNA sequencing results. Up-regulation of inflammation-associated genes: *Crispld2* (cysteine-rich secretory protein LCCL domain containing 2) and *Ccl20* (C-C motif chemokine ligand 20) (*E* and *F*). Abnormal expression of cell cycle checkpoint and migration genes: *Cks1b* (CDC28 protein kinase regulatory subunit 1B), *Agr2* (anterior gradient 2), *Slit2* (slit guidance ligand 2), and *Bcl2* (B cell lymphoma 2) (*C*, *D*, *H*, *I*). Up-regulation of downstream SMAD1/5 targets *Id1* (inhibitor of DNA binding 1) and *Id3* (inhibitor of DNA binding 3) (*A* and *B*), with down-regulation of upstream SMAD1/5-type 1 receptor *Acvr1* (activin A receptor type 1) (*G*). Down-regulation of steroid biosynthesis pathway genes: *Cyp51* (cytochrome p450 family 51 subfamily A member 1), *Cyp21a1* (cytochrome p450 family 21 subfamily A member1), *Ces1d* (carboxylesterase 1D precursor), and *Fdft1* (farnesyl diphosphate farnesyltransferase 1) (*J*–*M*). $*P \leq 0.05$; $**P \leq 0.01$; $***P \leq 0.001$.

of progesterone receptors that was noted in our study. With the epithelium unable to respond appropriately to the presence of progesterone to convert from a proliferative to secretory endometrium, uterine hyperplasia and tumor formation are imminent due to local unopposed estrogen (as confirmed by up-regulation of estrogen-responsive genes in our study). This proposed mechanism is further solidified by the fact that removal of ovaries at 6 wk in *Smad2/3* cKO mice prevented the loss of PR and the cancer phenotype, whereas by 12 wk, PR was already absent and tumor formation continued. Reintroducing estradiol into mice that were ovariectomized at 6 wk resulted in uterine hyperplasia, additionally confirming the estrogen-dependent uterine hyperplasia phenotype. Uterine cancer and its association with decreased expression of *PGR* has been well documented in human endometrial tumors (71, 72). In human endometrial cancer, *PGR* has been shown to be involved in cell cycle inhibition at the G1-to-S phase, as well as inhibition of tumor invasion (73), and *PGR* loss has been associated with higher metastatic potential and worse prognosis (74). However, the impact of *Smad2/3* on PR expression and metastasis has not previously been shown. Despite the importance of *PGR* in human cancers, the loss of *Pgr* expression is unlikely to be the sole driving force of tumor formation in the *Smad2/3* cKO mice, given that *Pgr* KO mice developed endometrial hyperplasia but not endometrial cancer (75).

An aberration in migration inflammatory markers could be a potential cause for the aggressiveness of these tumors. Our RNA sequencing analysis was performed at 6 wk of life and already showed significant differences in migratory (*Agr2* and *Slit2*) and inflammatory (*Ccl20* and *Crispld2*) markers between *Smad2/3* cKO and control mice. *Agr2*, which was up-regulated in the *Smad2/3* cKO mice, plays a role in cell migration, cellular transformation, and metastasis and is a p53 inhibitor (51–53, 76, 77). AGR2 increases aggressiveness of human endometrial cancer cells (54) and has even been suggested as a potential drug target for estrogen-responsive breast cancer (78). *Slit2*, down-regulated in *Smad2/3* cKO mice, inhibits cellular migration in the colon (79) and brain (80), with decreased levels being associated with more invasive tumors. The link between cancer and inflammation has been previously noted in several types of malignancies, including endometrial carcinoma (81). Estrogen has been associated with an inflammatory response (82), and, likewise, the proinflammatory environment has even been hypothesized to increase estrogen levels (83), further driving the cancer. *Ccl20*, one of the critical chemoattractants responsible for inflammatory cell recruitment, has been associated with multiple tumors, including those of the breast (84), lung (67), pancreas (85), and endometrium (86). This is consistent with previous studies showing that the TGF β pathway is a major player in cellular migration (87) and inflammation (37). *Crispld2* has been associated with antiinflammatory processes (67, 68); the significant up-regulation of *Crispld2*, a modulator of cytokine function, is indicative of an effort to counteract the otherwise inflammatory uterine milieu of our mouse model.

Another notable finding in our study is the significant increase in the expression of the *Id1–4* genes. Id proteins induce cell proliferation and inhibit cell differentiation and have been associated with different gynecological cancers (43–45). Id proteins are direct targets of bone morphogenetic proteins (BMPs) (88), which are activated by the BMP-activated SMAD1/5 pathway. TGF β (upstream of SMAD2/3) has been shown to bind to ALK1, activating SMAD1/5 to induce *Id* synthesis (89), and SMAD3 has even been shown to mediate transcriptional activation of *Id1* (90). This provides support that there is important countercommunication between the SMAD2/3 and SMAD1/5 pathways. This is solidified by the significant decrease in *Acvr1*/*Alk2* (a BMP-type 1 receptor that exclusively signals through SMAD1/5) in the *Smad2/3* cKO mice, indicating a negative feedback attempt (91) from the significant up-regulation of downstream SMAD1/5 genes. These results indicate that there is cross-talk and balance that occurs between the SMAD2/3 and SMAD1/5 signaling pathways. Antagonism between the SMAD1/5 and SMAD2/3 signaling pathways is frequently observed in other systems (46–48), including the ovary (92); in our model, inactivation of SMAD2/3 and resultant SMAD1/5 activation may drive tumorigenesis in the uterus. This is consistent with other studies indicating that SMAD2/3 serves a tumor suppressor role (93); however, the opposite has been shown to be true in the ovary (92, 94).

Several genes in the steroid/cholesterol biosynthesis pathway showed decreased mRNA expression levels (*Ces1d*, *Cyp51*, *Fdft1*, and *Cyp21a1*), likely as a result of aberrant estrogen feedback. While we do not believe that defects in steroidogenesis drive tumor formation in our model, we hypothesize that the decreased expression of several steroidogenic genes indicates an attempt to provide negative feedback to unopposed estrogen. This abnormal expression of steroid biosynthesis genes may provide insight into possible genes involved in estrogen metabolism and may serve as a useful biomarker for genetic susceptibility to endometrial cancer.

In this study, we show that SMAD2/3 serves an important tumor suppressor role in the TGF β pathway. Our findings not only generate a mouse model to study the role of SMAD2/3 in the uterus but also provide insight into the mechanism of uterine cancer and the potential for treatment development.

Materials and Methods

Animals. All mouse lines used in this study were maintained on a mixed C57BL/6/129S6/SvEv genetic background and handled under protocols approved by the Institutional Animal Care and Use Committee at Baylor College of Medicine.

Histological Analysis. Mouse uteri and ovaries were collected and fixed in 10% (vol/vol) neutral buffered formalin overnight. The specimens were then washed with 70% ethanol before being embedded in paraffin. Paraffin embedding was performed in the Pathology and Histology Core Facility at Baylor College of Medicine. Paraffin-embedded specimens were sectioned (5 μm thick). Paraffin sections were stained with H&E, PAS, or PAS-hematoxylin using standard procedures.

Immunohistochemistry and Immunofluorescence. Before staining, sections were deparaffinized and rehydrated in Histoclear (VWR); 100%, 90%, 80%, and 60% ethanol; and water. Antigen retrieval was performed by heating tissue sections in 10 mM sodium citrate and 0.05% Tween-20 (pH 6.0). For immunohistochemistry, after blocking with 3% (wt/vol) BSA for 1 h, sections were incubated with the primary antibodies overnight at 4 °C. Antibody information is listed in *SI Appendix*, Table S2. Sections were incubated with biotinylated secondary antibodies and ABC reagent (Vector Laboratories), and immunoreactive signals were developed using a 3,3′-diaminobenzidine substrate kit (Vector Laboratories) and counterstained with hematoxylin. Immunofluorescence used a similar protocol, except that the secondary antibody was Alexa Fluor 488 or Alexa Fluor 594 (both from Life Technologies). Quantification of Ki67 and PR was performed on immunohistochemistry slides by selecting three different portions of three control and cKO samples. Positively and negatively stained cells were then individually counted using ImageJ software (NIH).

RNA Isolation, qPCR, and RNA Sequencing Analysis. All tissues were frozen on dry ice immediately after collection. Total RNA was isolated using the RNeasy Mini Kit (Qiagen) by homogenizing the tissue with an OMNI-TH disrupter following the manufacturer's protocol. RNA (1–2 μg) was transcribed to cDNA using qScript cDNA Supermix (Quanta). Then, cDNA was used to amplify specific primers (listed in *SI Appendix*, Table S3). Gene expression was analyzed by qPCR with SYBR Green (Life Technologies/ABI) on a Roche 480 Light Cycler II. The relative fold change of a transcript was calculated by the delta delta cycle threshold ($2^{-\Delta\Delta CT}$) method as described previously (95) and analyzed using a Student *t* test. For RNA sequencing analysis, the raw reads were aligned to a mm10 reference genome by Tophat and assembled by Cufflinks. Expression values were quantile-normalized. Differential gene expression was assessed using a two-sided *t* test and fold change on log-transformed expression values. The method of Storey and Tibshirani (96) was used to estimate false discovery rates (FDRs) for nominally significant genes. For this dataset, a nominal $P < 0.01$ corresponded to an estimated FDR of 11.5%. Genes of interest were validated by qPCR. RNA sequencing data have been deposited in the Gene Expression Omnibus (accession no. GSE112664).

Hormone Analyses. Mice were anesthetized with isoflurane inhalation, and cardiac puncture was performed to collect the blood samples into serum separator tubes (BD). The serum was separated by centrifugation and stored at −20 °C until assayed for hormone levels. Serum FSH, LH, progesterone (P_4), and estradiol (E_2) were measured by the ligand assay and analysis core at the Center for Research in Reproduction, University of Virginia. The limit of detection of the assays is as follows: FSH (2 ng/mL), E_2 (10 pg/mL), LH (0.07 ng/mL), and P_4 (0.1 ng/mL).

Superovulation. As previously described (97), immature female mice (WT and $Smad2^{flox/-}$; $Smad3^{flox/-}$; $PR^{cre/+}$) were injected i.p. with 5 international units (IU) of pregnant mare serum gonadotropin (Calbiochem), followed by administration of 5 IU of human chorionic gonadotropin (hCG) (i.p.) 44–46 h later. After 18 h of hCG injection, the ovaries and oviducts were surgically removed and the cumulus oocyte complexes mass was recovered from the oviduct and collected into M2 medium (Sigma) containing 1 mg of hyaluronase per milliliter (Sigma) to dissociate the cumulus cells from oocytes. The numbers of oocytes were then counted and recorded.

Statistics. Comparison of means between two groups was conducted using a *t* test. Data are presented as mean ± SEM, and $P < 0.05$ was considered to be statistically significant.

ACKNOWLEDGMENTS. We thank Drs. Francesco J. DeMayo and John P. Lydon for the gift of the *Pgr-cre* mice and Yiquan Zhang for providing technical assistance. We acknowledge the University of Virginia core for analysis of our serum samples. These studies were supported by Eunice Kennedy Shriver National Institute of Child Health and Human Development Grants R01-HD032067 and R01-HD033438 (to M.M.M.), Grant K99-HD096057 (to D.M.), and Institutional Research and Academic Career Development Award K12-GM084897 (to D.M.). D.M. holds a Postdoctoral Enrichment Program Award from the Burroughs Wellcome Fund.

1. Chandra A, Copen CE, Stephen EH (2013) Infertility and impaired fecundity in the United States, 1982-2010: Data from the National Survey of Family Growth. *Natl Health Stat Report*, 1–18, 1 p following 19.
2. US Cancer Statistics Working Group (2018) US Cancer Statistics Data Visualizations Tool, based on November 2017 submission data (1999–2015) (US Department of Health and Human Services, Centers for Disease Control and Prevention and National Cancer Institute, Bethesda, MD). Available at https://www.cdc.gov/cancer/dataviz. Accessed March 1, 2018.
3. Gallos ID, et al. (2012) Regression, relapse, and live birth rates with fertility-sparing therapy for endometrial cancer and atypical complex endometrial hyperplasia: A systematic review and metaanalysis. *Am J Obstet Gynecol* 207:266.e1–266.e12.
4. Ushijima K, et al. (2007) Multicenter phase II study of fertility-sparing treatment with medroxyprogesterone acetate for endometrial carcinoma and atypical hyperplasia in young women. *J Clin Oncol* 25:2798–2803.
5. Gunderson CC, Fader AN, Carson KA, Bristow RE (2012) Oncologic and reproductive outcomes with progestin therapy in women with endometrial hyperplasia and grade 1 adenocarcinoma: A systematic review. *Gynecol Oncol* 125:477–482.
6. Ramirez PT, Frumovitz M, Bodurka DC, Sun CC, Levenback C (2004) Hormonal therapy for the management of grade 1 endometrial adenocarcinoma: A literature review. *Gynecol Oncol* 95:133–138.
7. Qin Y, et al. (2016) Oral progestin treatment for early-stage endometrial cancer: A systematic review and meta-analysis. *Int J Gynecol Cancer* 26:1081–1091.
8. Giudice LC (1994) Growth factors and growth modulators in human uterine endometrium: Their potential relevance to reproductive medicine. *Fertil Steril* 61:1–17.
9. Rutanen EM (1998) Insulin-like growth factors in endometrial function. *Gynecol Endocrinol* 12:399–406.
10. Guzeloglu-Kayisli O, Kayisli UA, Taylor HS (2009) The role of growth factors and cytokines during implantation: Endocrine and paracrine interactions. *Semin Reprod Med* 27:62–79.
11. Nelson KG, Takahashi T, Bossert NL, Walmer DK, McLachlan JA (1991) Epidermal growth factor replaces estrogen in the stimulation of female genital-tract growth and differentiation. *Proc Natl Acad Sci USA* 88:21–25.
12. Byron SA, et al. (2008) Inhibition of activated fibroblast growth factor receptor 2 in endometrial cancer cells induces cell death despite PTEN abrogation. *Cancer Res* 68:6902–6907.
13. Dong J, et al. (1996) Growth differentiation factor-9 is required during early ovarian folliculogenesis. *Nature* 383:531–535.
14. Li Q, et al. (2008) Redundant roles of SMAD2 and SMAD3 in ovarian granulosa cells in vivo. *Mol Cell Biol* 28:7001–7011.
15. Fullerton PT, Jr, Monsivais D, Kommagani R, Matzuk MM (2017) Follistatin is critical for mouse uterine receptivity and decidualization. *Proc Natl Acad Sci USA* 114:E4772–E4781.
16. Lee KY, et al. (2007) Bmp2 is critical for the murine uterine decidual response. *Mol Cell Biol* 27:5468–5478.
17. Peng J, et al. (2015) Uterine activin receptor-like kinase 5 is crucial for blastocyst implantation and placental development. *Proc Natl Acad Sci USA* 112:E5098–E5107.
18. Clementi C, et al. (2013) Activin-like kinase 2 functions in peri-implantation uterine signaling in mice and humans. *PLoS Genet* 9:e1003863.

19. Peng J, et al. (2015) Uterine activin-like kinase 4 regulates trophoblast development during mouse placentation. *Mol Endocrinol* 29:1684–1693.
20. Li Q (2014) Transforming growth factor β signaling in uterine development and function. *J Anim Sci Biotechnol* 5:52.
21. Gao Y, et al. (2015) Constitutive activation of transforming growth factor Beta receptor 1 in the mouse uterus impairs uterine morphology and function. *Biol Reprod* 92:34.
22. Li Q, Graff JM, O'Connor AE, Loveland KL, Matzuk MM (2007) SMAD3 regulates gonadal tumorigenesis. *Mol Endocrinol* 21:2472–2486.
23. Piestrzeniewicz-Ulanska D, et al. (2004) TGF-β signaling is disrupted in endometrioid-type endometrial carcinomas. *Gynecol Oncol* 95:173–180.
24. Fleming NI, et al. (2013) SMAD2, SMAD3 and SMAD4 mutations in colorectal cancer. *Cancer Res* 73:725–735.
25. Pangas SA, et al. (2008) Conditional deletion of Smad1 and Smad5 in somatic cells of male and female gonads leads to metastatic tumor development in mice. *Mol Cell Biol* 28:248–257.
26. Li Q, et al. (2011) Transforming growth factor β receptor type 1 is essential for female reproductive tract integrity and function. *PLoS Genet* 7:e1002320.
27. Gao Y, Lin P, Lydon JP, Li Q (2017) Conditional abrogation of transforming growth factor-β receptor 1 in PTEN-inactivated endometrium promotes endometrial cancer progression in mice. *J Pathol* 243:89–99.
28. Parekh TV, et al. (2002) Transforming growth factor β signaling is disabled early in human endometrial carcinogenesis concomitant with loss of growth inhibition. *Cancer Res* 62:2778–2790.
29. Piestrzeniewicz-Ulanska D, Brys M, Semczuk A, Jakowicki JA, Krajewska WM (2002) Expression of TGF-beta type I and II receptors in normal and cancerous human endometrium. *Cancer Lett* 186:231–239.
30. Ungefroren H, et al. (2011) Differential roles of Smad2 and Smad3 in the regulation of TGF-β1-mediated growth inhibition and cell migration in pancreatic ductal adenocarcinoma cells: Control by Rac1. *Mol Cancer* 10:67.
31. Heyer J, et al. (1999) Postgastrulation Smad2-deficient embryos show defects in embryo turning and anterior morphogenesis. *Proc Natl Acad Sci USA* 96: 12595–12600.
32. Nomura M, Li E (1998) Smad2 role in mesoderm formation, left-right patterning and craniofacial development. *Nature* 393:786–790.
33. Yang X, et al. (1999) Targeted disruption of SMAD3 results in impaired mucosal immunity and diminished T cell responsiveness to TGF-beta. *EMBO J* 18:1280–1291.
34. Zhu Y, Richardson JA, Parada LF, Graff JM (1998) Smad3 mutant mice develop metastatic colorectal cancer. *Cell* 94:703–714.
35. Soyal SM, et al. (2005) Cre-mediated recombination in cell lineages that express the progesterone receptor. *Genesis* 41:58–66.
36. Liu Y, et al. (2004) Smad2 and Smad3 coordinately regulate craniofacial and endodermal development. *Dev Biol* 270:411–426.
37. Takimoto T, et al. (2010) Smad2 and Smad3 are redundantly essential for the TGF-beta-mediated regulation of regulatory T plasticity and Th1 development. *J Immunol* 185:842–855, and erratum (2011) 186:632.
38. Liu Y, Festing MH, Hester M, Thompson JC, Weinstein M (2004) Generation of novel conditional and hypomorphic alleles of the Smad2 gene. *Genesis* 40:118–123.
39. Matzuk MM, Kumar TR, Bradley A (1995) Different phenotypes for mice deficient in either activins or activin receptor type II. *Nature* 374:356–360.
40. Hendzel MJ, et al. (1997) Mitosis-specific phosphorylation of histone H3 initiates primarily within pericentromeric heterochromatin during G2 and spreads in an ordered fashion coincident with mitotic chromosome condensation. *Chromosoma* 106: 348–360.
41. Gerdes SJ, et al. (1984) Cell cycle analysis of a cell proliferation-associated human nuclear antigen defined by the monoclonal antibody Ki-67. *J Immunol* 133:1710–1715.
42. Bokhman JV (1983) Two pathogenetic types of endometrial carcinoma. *Gynecol Oncol* 15:10–17.
43. Maw MK, Fujimoto J, Tamaya T (2009) Overexpression of inhibitor of DNA-binding (ID)-1 protein related to angiogenesis in tumor advancement of ovarian cancers. *BMC Cancer* 9:430.
44. Maw MK, Fujimoto J, Tamaya T (2010) Role of inhibitor of DNA binding-1 protein is related to angiogenesis in the tumor advancement of uterine endometrial cancers. *Exp Ther Med* 1:351–356.
45. Maw MK, Fujimoto J, Tamaya T (2008) Expression of the inhibitor of DNA-binding (ID)-1 protein as an angiogenic mediator in tumour advancement of uterine cervical cancers. *Br J Cancer* 99:1557–1563.
46. Matsumoto Y, et al. (2012) Bone morphogenetic protein-3b (BMP-3b) inhibits osteoblast differentiation via Smad2/3 pathway by counteracting Smad1/5/8 signaling. *Mol Cell Endocrinol* 350:78–86.
47. Amarnath S, Agarwala S (2017) Cell-cycle-dependent TGFβ-BMP antagonism regulates neural tube closure by modulating tight junctions. *J Cell Sci* 130:119–131.
48. Eickelberg O, Morty RE (2007) Transforming growth factor beta/bone morphogenic protein signaling in pulmonary arterial hypertension: Remodeling revisited. *Trends Cardiovasc Med* 17:263–269.
49. Wong K, Park HT, Wu JY, Rao Y (2002) Slit proteins: Molecular guidance cues for cells ranging from neurons to leukocytes. *Curr Opin Genet Dev* 12:583–591.
50. Adams JM, Cory S (1998) The Bcl-2 protein family: Arbiters of cell survival. *Science* 281: 1322–1326.
51. Wang Z, Hao Y, Lowe AW (2008) The adenocarcinoma-associated antigen, AGR2, promotes tumor growth, cell migration, and cellular transformation. *Cancer Res* 68:492–497.
52. Park K, et al. (2011) AGR2, a mucinous ovarian cancer marker, promotes cell proliferation and migration. *Exp Mol Med* 43:91–100.
53. Di Maro G, et al. (2014) Anterior gradient protein 2 promotes survival, migration and invasion of papillary thyroid carcinoma cells. *Mol Cancer* 13:160.
54. Hrstka R, et al. (2017) Tamoxifen-dependent induction of *AGR2* is associated with increased aggressiveness of endometrial cancer cells. *Cancer Invest* 35: 313–324.
55. Tang Y, Reed SI (1993) The Cdk-associated protein Cks1 functions both in G1 and G2 in Saccharomyces cerevisiae. *Genes Dev* 7:822–832.
56. Martinsson-Ahlzén H-S, et al. (2008) Cyclin-dependent kinase-associated proteins Cks1 and Cks2 are essential during early embryogenesis and for cell cycle progression in somatic cells. *Mol Cell Biol* 28:5698–5709.
57. Hadwiger JA, Wittenberg C, Mendenhall MD, Reed SI (1989) The Saccharomyces cerevisiae CKS1 gene, a homolog of the Schizosaccharomyces pombe suc1+ gene, encodes a subunit of the Cdc28 protein kinase complex. *Mol Cell Biol* 9: 2034–2041.
58. Miller WL, Auchus RJ (2011) The molecular biology, biochemistry, and physiology of human steroidogenesis and its disorders. *Endocr Rev* 32:81–151.
59. Huhtinen K, et al. (2012) Endometrial and endometriotic concentrations of estrone and estradiol are determined by local metabolism rather than circulating levels. *J Clin Endocrinol Metab* 97:4228–4235.
60. Lepesheva GI, Waterman MR (2004) CYP51–the omnipotent P450. *Mol Cell Endocrinol* 215:165–170.
61. Dempsey ME (1974) Regulation of steroid biosynthesis. *Annu Rev Biochem* 43: 967–990.
62. Papackova Z, Cahova M (2015) Fatty acid signaling: The new function of intracellular lipases. *Int J Mol Sci* 16:3831–3855.
63. Yang L, Pang Y, Moses HL (2010) TGF-β and immune cells: An important regulatory axis in the tumor microenvironment and progression. *Trends Immunol* 31: 220–227.
64. Yoshimura A, Muto G (2011) TGF-β function in immune suppression. *Curr Top Microbiol Immunol* 350:127–147.
65. Shull MM, et al. (1992) Targeted disruption of the mouse transforming growth factor-beta 1 gene results in multifocal inflammatory disease. *Nature* 359:693–699.
66. Beider K, et al. (2009) Interaction between CXCR4 and CCL20 pathways regulates tumor growth. *PLoS One* 4:e5125.
67. Zhang H, et al. (2016) CRISPLD2 (LGL1) inhibits proinflammatory mediators in human fetal, adult, and COPD lung fibroblasts and epithelial cells. *Physiol Rep* 4: e12942.
68. Yoo JY, et al. (2014) CRISPLD2 is a target of progesterone receptor and its expression is decreased in women with endometriosis. *PLoS One* 9:e100481.
69. Uhlen M, et al. (2017) A pathology atlas of the human cancer transcriptome. *Science* 357:eaan2507.
70. Ito I, et al. (2010) Estrogen inhibits transforming growth factor β signaling by promoting Smad2/3 degradation. *J Biol Chem* 285:14747–14755.
71. Arnett-Mansfield RL, et al. (2001) Relative expression of progesterone receptors A and B in endometrioid cancers of the endometrium. *Cancer Res* 61:4576–4582.
72. Fujimoto J, Ichigo S, Hori M, Nishigaki M, Tamaya T (1995) Expression of progesterone receptor form A and B mRNAs in gynecologic malignant tumors. *Tumour Biol* 16: 254–260.
73. Dai D, Wolf DM, Litman ES, White MJ, Leslie KK (2002) Progesterone inhibits human endometrial cancer cell growth and invasiveness: Down-regulation of cellular adhesion molecules through progesterone B receptors. *Cancer Res* 62:881–886.
74. Trovik J, et al.; MoMaTEC study group (2013) Hormone receptor loss in endometrial carcinoma curettage predicts lymph node metastasis and poor outcome in prospective multicentre trial. *Eur J Cancer* 49:3431–3441.
75. Lydon JP, et al. (1995) Mice lacking progesterone receptor exhibit pleiotropic reproductive abnormalities. *Genes Dev* 9:2266–2278.
76. Hrstka R, et al. (2016) AGR2 oncoprotein inhibits p38 MAPK and p53 activation through a DUSP10-mediated regulatory pathway. *Mol Oncol* 10:652–662.
77. Pohler E, et al. (2004) The Barrett's antigen anterior gradient-2 silences the p53 transcriptional response to DNA damage. *Mol Cell Proteomics* 3:534–547.
78. Salmans ML, Zhao F, Andersen B (2013) The estrogen-regulated anterior gradient 2 (AGR2) protein in breast cancer: A potential drug target and biomarker. *Breast Cancer Res* 15:204.
79. Chen WF, et al. (2013) SLIT2 inhibits cell migration in colorectal cancer through the AKT-GSK3β signaling pathway. *Int J Colorectal Dis* 28:933–940.
80. Yiin J-J, et al. (2009) Slit2 inhibits glioma cell invasion in the brain by suppression of Cdc42 activity. *Neuro Oncol* 11:779–789.
81. Wallace AE, Gibson DA, Saunders PTK, Jabbour HN (2010) Inflammatory events in endometrial adenocarcinoma. *J Endocrinol* 206:141–157.
82. Monteiro R, Teixeira D, Calhau C (2014) Estrogen signaling in metabolic inflammation. *Mediators Inflamm* 2014:615917.
83. Modugno F, Ness RB, Chen C, Weiss NS (2005) Inflammation and endometrial cancer: A hypothesis. *Cancer Epidemiol Biomarkers Prev* 14:2840–2847.
84. Marsigliante S, Vetrugno C, Muscella A (2013) CCL20 induces migration and proliferation on breast epithelial cells. *J Cell Physiol* 228:1873–1883.
85. Liu B, et al. (2016) Tumor-associated macrophage-derived CCL20 enhances the growth and metastasis of pancreatic cancer. *Acta Biochim Biophys Sin (Shanghai)* 48: 1067–1074.
86. Liu Y, et al. (2016) CCL20 mediates RANK/RANKL-induced epithelial-mesenchymal transition in endometrial cancer cells. *Oncotarget* 7:25328–25339.
87. Massagué J (1998) TGF-beta signal transduction. *Annu Rev Biochem* 67:753–791.
88. Hollnagel A, Oehlmann V, Heymer J, Rüther U, Nordheim A (1999) Id genes are direct targets of bone morphogenetic protein induction in embryonic stem cells. *J Biol Chem* 274:19838–19845.
89. Miyazono K, Miyazawa K (2002) Id: A target of BMP signaling. *Sci STKE* 2002: pe40.

90. Liang YY, Brunicardi FC, Lin X (2009) Smad3 mediates immediate early induction of Id1 by TGF-β. *Cell Res* 19:140–148.
91. Miyazono K (2000) Positive and negative regulation of TGF-beta signaling. *J Cell Sci* 113:1101–1109.
92. Middlebrook BS, Eldin K, Li X, Shivasankaran S, Pangas SA (2009) Smad1-Smad5 ovarian conditional knockout mice develop a disease profile similar to the juvenile form of human granulosa cell tumors. *Endocrinology* 150:5208–5217.
93. Samanta D, Datta PK (2012) Alterations in the Smad pathway in human cancers. *Front Biosci (Landmark Ed)* 17:1281–1293.
94. Edson MA, et al. (2010) Granulosa cell-expressed BMPR1A and BMPR1B have unique functions in regulating fertility but act redundantly to suppress ovarian tumor development. *Mol Endocrinol* 24:1251–1266.
95. Livak KJ, Schmittgen TD (2001) Analysis of relative gene expression data using real-time quantitative PCR and the 2(-Delta Delta C(T)) method. *Methods* 25:402–408.
96. Storey JD, Tibshirani R (2003) Statistical significance for genomewide studies. *Proc Natl Acad Sci USA* 100:9440–9445.
97. Pangas SA, et al. (2007) Intraovarian activins are required for female fertility. *Mol Endocrinol* 21:2458–2471.